Effect of Interfacial Waves on Turbulence Structure in Stratified Duct Flows

M. Fernandino
e-mail: maria.fernandino@ntnu.no

T. Ytrehus

Department of Energy and Process Engineering,
Norwegian University of Science and Technology,
N-7491 Trondheim, Norway

Stratified flows are encountered in many industrial applications. The determination of the flow characteristics is essential for the prediction of pressure drop and holdup in the system. The aim of this study is to gain insight into the interaction of a gas and a liquid phase flowing in a stratified regime, with especial focus on the effect of interfacial waves on the turbulence structure of the liquid phase. Measurements of mean velocities and turbulent intensities in the liquid phase of a stratified air-water duct flow are performed. Mean velocity profiles and turbulence structure are affected differently for different wave amplitudes. The effect of small amplitude waves is restricted to the near-interface region, resembling the effect of increasing shear rate on a flat interface. On the other hand, large amplitude waves modify the flow structure throughout the whole liquid depth. The mean velocity is greatly enhanced, resulting in a higher bulk velocity. Turbulent intensities are also significantly enhanced especially in the interface region. This big difference in flow structure is not observed after the appearance of the first waves but rather when a certain critical wave amplitude is triggered, indicating that the prediction of this critical wave type turns out to be more important than the determination of the transition from a smooth to a stratified wavy regime. [DOI: 10.1115/1.2928295]

1 Introduction

Contrary to turbulence in the wall region, which has been intensively studied over the past two decades, turbulence near fluid-fluid interfaces has not been studied with the same detail due to the difficulties that lie on the measurements near this interface and on the simulation of flows with deformable interfaces. With the accessibility of new experimental techniques, such as laser Doppler velocimetry (LDV), more and more data of the flow structure close to gas-liquid interfaces are now becoming available.

Free-surface flows have been studied experimentally and numerically. In the LDV experiments from Nezu and Rodi [1], the mean velocity profile was found to deviate from the logarithmic behavior near the free surface (for $\mathrm{Re}_h > 10{,}000$). According to the authors, as the Reynolds number becomes larger, such deviation cannot be neglected for $y/h_L > 0.6$, and they suggested the use of the Coles wake law as the more convenient way to account for this deviation. Contrary to the findings of Nezu and Rodi [1], Rashidi and Banerjee [2] did not observe any deviation from the logarithmic law near the interface. They attributed this fact to the lower Reynolds numbers that were used in their study as compared to those in the work of Nezu and Rodi [1]. Near a shear-free surface, vertical fluctuations are damped due to gravity and surface tension, resembling the behavior of a solid boundary. At the same time, streamwise and spanwise fluctuations are enhanced in the interfacial region [2,3]. The direct numerical simulation (DNS) of free-surface flows performed by Komori et al. [4] and Pan and Banerjee [5] confirm these experimental results.

When an interfacial shear is applied, the interface region becomes an active one, where structures can form and even attach to the interface as opposed to what happens at a solid wall [6–8]. For low shear rates, bursts coming from the wall region are responsible for scalar transport, whereas for high enough shear rates, the fluid structures originating in the interface region dominate the process.

Under the condition of small shear rates, small amplitude (SA) waves form on the interface. SA disturbances do not significantly influence the flow structure, and the interface can be treated as a rigid slip wall in numerical simulations [4,8]. This is because in this case, the shear rate appears to be more important than the nature of the boundary conditions in determining such structures [7]. For this case of small disturbances, the mean velocity profile follows the logarithmic law near the wall, with higher values of the summation constant A with increasing interfacial shear [7]. The mean velocity profiles from and near the sheared interface also follow a logarithmic profile from the center of the flow up to $y_i^+ \approx 20-30$ according to the experimental study of Rashidi and Banerjee [7]. No outer region was seen to exist since both logarithmic regions (wall and interface) interact with each other.

When significant shear is imposed on the liquid surface, the surface is no longer "free" and entirely different structures result. The presence of larger amplitude interfacial waves changes the kinematic and turbulence structure of the liquid phase close to the sheared interface (see, for example, Ref. [9]). Fabre et al. [10] observed an increase in turbulent intensities close to the wavy interface. However, no description of the wave structure was provided. Streamwise and vertical turbulent fluctuations were also seen to increase substantially under the presence of waves by Kemp and Simons [11]. Rashidi et al. [12] superimposed SA gravity waves on a turbulent liquid layer via a wave maker, with a maximum wave amplitude to liquid film height ratio of $h_w/h_L = 0.16$. For an increasing wave amplitude, the value of the wall shear velocity u_τ was seen to increase under wave crests and to decrease under wave troughs, resulting in a nearly constant mean value. Mean velocities were seen to be higher near the interface and near the wall for an increasing wave amplitude, and, therefore, a small deviation from the logarithmic law was observed for those cases. Similar observations were reported by Kemp and Simons [11]. The intensity of turbulent fluctuations showed a similar behavior as in free-surface flows although their intensity was increased by the presence of superficial waves. The frequency of bursts originating at the wall was increased by the occurrence of waves, implying that the transport of turbulent energy from the wall to the interface region was altered when waves were present. Reynolds stresses in the wall region were amplified also due to the

Contributed by the Fluids Engineering Division of ASME for publication in the JOURNAL OF FLUIDS ENGINEERING. Manuscript received August 29, 2006; final manuscript received March 11, 2008; published online May 19, 2008. Assoc. Editor Phillip M. Ligrani.

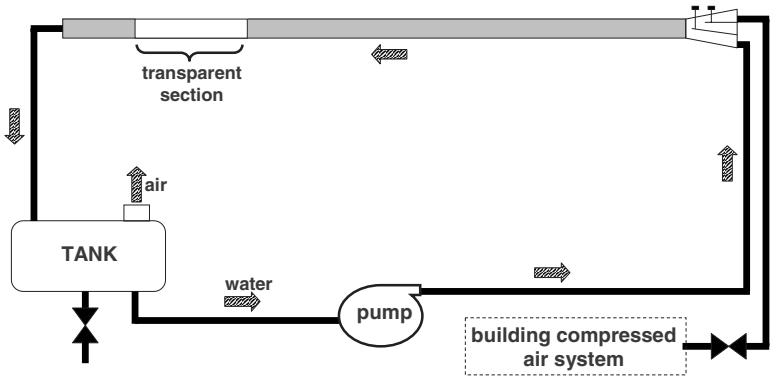

Fig. 1 Experimental facility

change in wall ejection frequency. These effects would be more important for the large amplitude (LA) waves usually found in stratified flows in industrial applications.

Interfacial waves are also known to induce secondary currents both in the gas and the liquid phase of a stratified flow, having important effects on the flow structure in each of the two phases [13–15]. The variation in wave amplitude across the width of the duct is an important source for the mean secondary flow [15]. The measurements in duct flow from Suzanne [13] show two counter-rotating vortices in the duct cross-section area in the liquid phase. The flow goes up along the lateral walls and comes down along the duct center plane. This flow is responsible for the maximum streamwise velocity occurring just below the interface. Similar secondary motions were reported in the numerical simulations of a rectangular duct flow by Nordsveen [15] and the pipe flow measurements of Andreussi and Persen [16]. For a duct aspect ratio of 6, Nordsveen [15] reported that wave-induced secondary currents were much more important than turbulence-induced ones. The former formed in all the duct cross-section areas (but mainly along the interface), and the latter only close to the walls and corners. For an aspect ratio of 2, both effects were of the same order.

Even when the number of results reported in the literature regarding wave-turbulence interaction has increased during the past years, much work still needs to be done before we can really understand the dynamics of interaction and transport phenomena occurring between a gas and a liquid flowing in a stratified regime. In particular, the effect of LA waves on turbulence structure has not been largely documented in the literature, mainly due to the difficulties involved both in numerical simulations and in laboratory measurements. Furthermore, while some authors claim to have studied LA wave effect on a flow structure, we have not found any work where the ratio of wave amplitude to liquid film height was as large as the one considered in this work. In this work, wave-turbulence interaction in a stratified air-water duct flow is studied. LDV measurements of mean velocity and turbulence structure in the liquid phase for different kinds of interfacial waves are presented. A comparison of LA waves and liquid film heights is included in this study.

2 Description of the Experiments

The experiments were carried out in a horizontal 9 m long duct, with a square cross-section area of 7×7 cm^2. The duct was made of stainless steel, and an acrylic transparent section was introduced approximately 6 m from the entrance, where velocity measurements were performed. Figure 1 shows a schematic diagram of the flow loop.

The study was performed using air and water at atmospheric pressure as working fluids. The duct inlet had three entrances intended for the injection of gas, water, and oil into the duct. Water was injected through the bottom entrance, and air through the top one. The air was supplied by the laboratory compressed-air system and was regulated by a manual valve. The water was recirculated by a manually regulated screw pump from a tank connected to the outlet of the channel. The water flow rate was monitored by an electromagnetic flow meter, and the air flow rate by a mass flow meter operating on the principle of heat transfer along a laminar flow device. Both fluids entered the channel through a square–cross-section converging nozzle with two inlets, one above the other (see Fig. 1). The water was introduced through the bottom of the nozzle, and the air through the top half.

The pressure drop along the channel and the test section was measured using a double positive dp-cell. A Pt100 probe placed at the end of the transparent test section was used to record the temperature of the water phase.

Measurements of the liquid velocity and turbulent fluctuations were performed using LDV. The laser used was a TSI two-component argon-ion laser with wavelengths of 514.4 nm and 488.0 nm. The laser was mounted on a traverse mechanism capable of shifting positions in the vertical and horizontal (streamwise) directions. It was pointing at the transparent section perpendicularly from the side of the duct.

The measurements were performed for liquid superficial velocities of $U_{LS}=0.068$ m/s and $U_{LS}=0.136$ m/s, resulting in mean liquid heights of $h_L=21$ mm and $h_L=31$ mm, respectively. The gas superficial velocities were varied from 0 m/s to 3.5 m/s. The parameters for each measured case are shown in Table 1. The laser was aimed at the center plane of the duct from the side. In order to ensure the two dimensionality of the measurements, the laser was aligned by measuring the distance from the laser outer diameter (from two opposite points of its diameter, pointing upstream and downstream from the measuring point) to the lateral wall of the duct. Velocity measurements were performed in the liquid phase throughout the whole liquid film depth.

Laser data acquisition was made simultaneously in both channels, thus being able to directly measure Reynolds stresses. Near the interface and near the wall, the beams corresponding to the vertical velocity measurements were obstructed by the bottom wall or were above the water surface. Therefore, the acquisition was no longer simultaneous in both channels, resulting in measurements only of streamwise velocity components in these regions.

During the velocity measurements, interfacial waves were characterized by the spectra obtained from the LDV measurement of vertical fluctuations close to the interface. The method is described in detail in Fernandino and Ytrehus [17]. Basically, three subregimes were identified with this method and will be considered in this work: (i) stratified smooth (SS) waves, (ii) SA waves, and (iii) 2D LA waves (two dimensional at the centerline of the duct, away from the lateral walls). The SS regime is characterized by a flat spectrum. In turn, the SA regime presented one dominant frequency at 12–14 Hz. Two dominant frequencies (two peaks)

Table 1 Combination of air and water flow rates used during this study, with U_{LS} as the water superficial velocity, U_L the mean water velocity, h_L the mean liquid film height and corresponding Reynolds number Re_L based on the mean velocity and mean liquid depth, U_{GS} the gas superficial velocity, Re_{GS} the gas phase Reynolds number based on the superficial, velocity, and h_w the mean wave amplitude. The SS, SA, and LA (wave regimes) are classified according to Fernandino and Ytrehus [17].

	U_{LS} (m/s)	U_L (m/s)	h_L (mm)	Re_L	U_{GS} (m/s)	Re_{GS}	h_w (mm)
Run 2a	0.068	0.34	21	7140	0	0	0 (SS)
Run 2b	0.068	0.34	21	7140	1.24	5748	0 (SS)
Run 2c	0.068	0.34	21	7140	1.69	7834	~1 (SS)
Run 2d	0.068	0.34	21	7140	1.83	8483	2–3 (SA)
Run 2e	0.068	0.34	21	7140	1.96	9086	2–4 (SA)
Run 2f	0.068	0.35	21	7350	2.19	10,152	4–5 (SA)
Run 2g	0.068	0.35	21	7350	2.53	11,728	5–6 (SA)
Run 2h	0.068	0.38	21	7980	2.92	13,536	8–10 (LA)
Run 2i	0.068	0.41	21	8610	3.25	15,066	~10 (LA)
Run 3a	0.136	0.44	31	13,640	0	0	0 (SS)
Run 3b	0.136	0.47	31	14,570	1.23	5702	1–2 (SA)
Run 3c	0.136	0.48	31	14,880	1.72	7973	4–6 (SA)
Run 3d	0.136	0.48	31	14,880	2.21	10,245	7–9 (LA)
Run 3e	0.136	0.48	31	14,880	2.41	11,172	9–10 (LA)
Run 3f	0.136	0.53	31	16,430	2.87	13,305	~10 (LA)
Run 3g	0.136	0.60	31	18,600	3.31	15,344	10–12 (LA)

appeared in the spectrum when the air flow was further increased and led the way almost immediately to one dominant frequency, this time at 7 Hz. The latter was designated as the LA waves. Mean velocities and turbulent fluctuations were characterized based on this subregime classification.

3 Results and Discussion

3.1 Mean Velocity. Mean velocities and turbulent fluctuations presented in this section are nondimensionalized with the wall shear velocity $u_\tau \equiv \sqrt{\tau_w/\rho_L}$, with τ_w as the mean wall shear stress and ρ_L the liquid density. Different methods for obtaining the wall shear velocity were analyzed, namely, obtaining the wall shear velocity from the velocity gradient at the wall, from the measured mean velocity profile and the logarithmic law, from the measured pressure drop, from the measured Reynolds stresses, and from the expression $\tau_w = f_L \rho_L U_L^2/2$ and the Blasius formula $f_L = 0.0559 Re_L^{-0.22}$, with f_L as the liquid wall friction factor (the methods were described and compared in detail in Ref. [18]). The latter option seemed to be the most appropriate and is the one used in this work.

Figure 2 shows the measured mean velocity profile for a free-surface condition. Here, $y^+ = y u_\tau/\nu_L$, where y represents the distance from the wall. The profile presents a logarithmic region for $y^+ \geqslant 70$, in accordance with the empirical log law for an open channel flow, with the von Karman's constant $\kappa = 0.41$ and the summation constant $A = 5.5$ [1,2]. A small deviation from the logarithmic behavior is observed close to the interface for Run 2a for $y/h_L \geqslant 0.8$. For Run 3a, the deviation is more significant and the profile shows a zero shear region close to the interface.

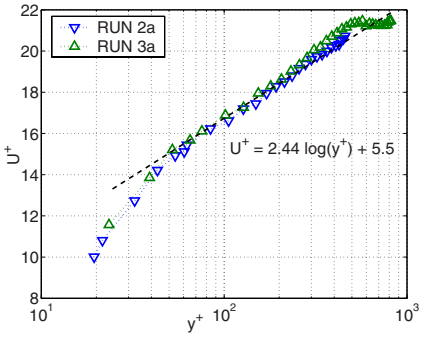

Fig. 2 The measured mean velocity profile for the free-surface duct flow compared to the empirical log law of the wall for the open channel flow

Mean velocity profiles for different air superficial velocities are shown in Fig. 3. The horizontal black lines indicate the mean interface level. The dashed line is the mean level corresponding to the more wavy interfaces, where the position of the interface could not be located accurately but just visually (the wave amplitude varied throughout the duct width). Therefore, the profiles from Run 2f and Run 3d onward show the same mean water level. The filled rounded dots in Fig. 3 indicate the reference free-surface profile (Runs 2a and 3a).

As the air flow is increased (always by the same constant amount), the velocity profiles are enhanced close to the interface, while the rest of the bulk flow is nearly undisturbed (Runs 2b–2e and 3a–3c). In these cases, the result of increasing the interfacial shear rate translates into increasing the profile slope close to the sheared surface only. However, if the air flow is increased a little more (Runs 2f and 2g and 3d and 3e), the velocity in the bulk region of the flow is also increased, forming a kind of belly in the profile in that region. For higher air flows (Runs 2h and 2i and 3f and 3g), mean velocities are enhanced near the interface and near the wall as well, while they seem to decrease in the center region with respect to the wall and interface values, resulting in an s-shaped profile. This s-shaped velocity profile accompanied by a significant increase in bulk velocity was also observed by Suzanne [13] during rectangular duct flow measurements and by Strand [14] during stratified pipe flow experiments. This means that the s-shaped profile with higher bulk velocity is not a consequence of the rectangular cross section but of the flow itself. It is worth remembering here that the s-shaped profile was observed (both in this work and in the mentioned previous studies) in the duct/pipe centerline. As one comes close to the lateral walls of the duct or the point of contact of the liquid film with the walls of the pipe, it is expected that the flow in those regions could experience some backward recirculations caused by the direct interaction of the waves with the solid walls. Some three-dimensional effects from the lateral walls are also expected for the studied liquid film height to duct width ratio.

It can be seen that the effect of a shear imposed on the interface is restricted to the near-interface region only for low shear rates.

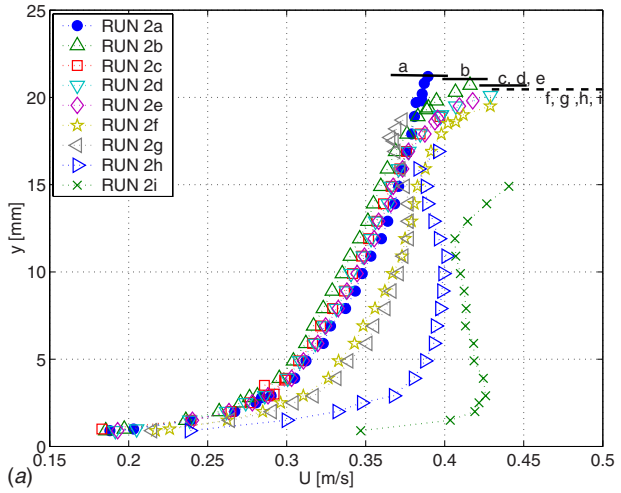

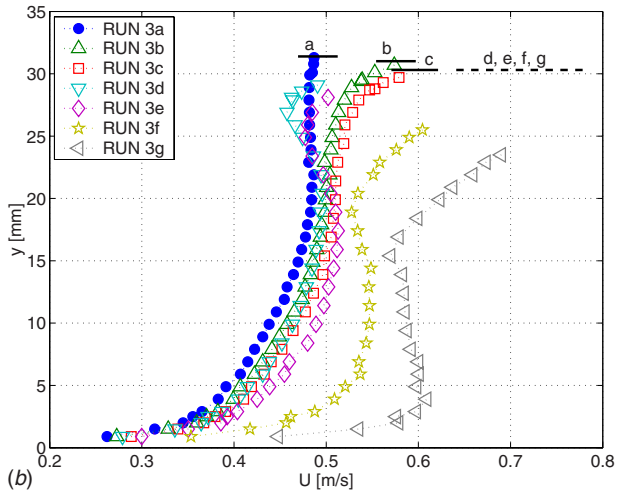

Fig. 3 Mean streamwise velocity profiles for different air superficial velocities and corresponding wave patterns: (*a*) Run 2 and (*b*) Run 3. The black lines indicate the interface position.

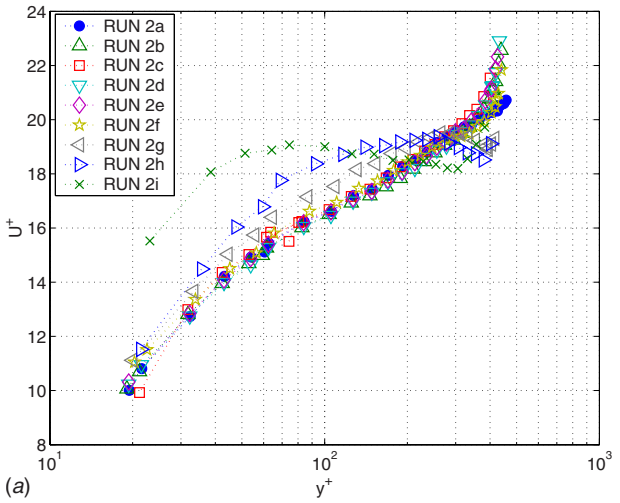

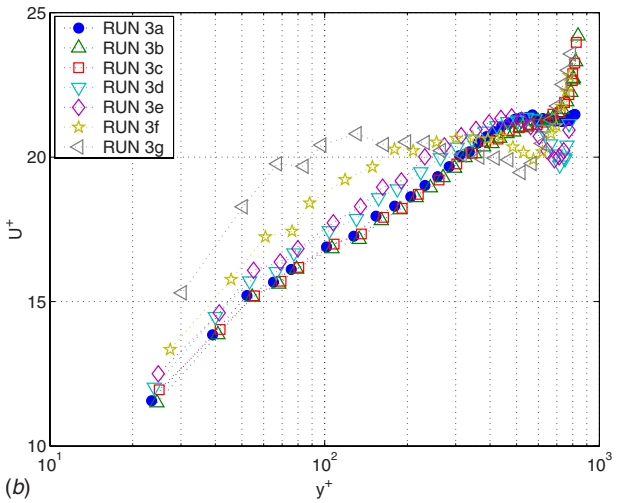

Fig. 4 Nondimensional mean stremaiwse velocity profiles for different air superficial velocities and corresponding wave patterns: (*a*) Run 2 and (*b*) Run 3

On the other hand, for a sufficiently high shear rate, the shape of the mean velocity profiles is affected also in the bulk region of the flow, while the near wall region seems to remain unaltered. When the shear is enough to trigger the appearance of LA waves on the interface, an s-shaped profile and an apparent significant increase in the liquid bulk velocity is observed.

Figure 4 shows the same profiles as in Fig. 3, but they are nondimensionalized with the inner variables ν_L and shear velocity u_τ. The profiles corresponding to free-surface flow are plotted with filled dots. In all cases, a deviation from the logarithmic profile is observed near the interface. However, for $50 < y^+ < 200$, almost all profiles coincide with the empirical logarithmic law for the open channel flow, except the ones corresponding to LA waves on the interface (Runs 2h and 2i and 3f and 3g). Regarding Runs 2g and 3d and 3e, a logarithmic region seems to exist although the summation constant appears to be larger.

The large increase in bulk velocity when LA waves appear on the interface indicates an overall decrease in wall shear and corresponds to a significant increase in pressure drop in the gas phase [17]. It is not clear from these measurements why the velocity profile is shifted so much to the front. One hypothesis is related to the effect of drag reduction. Waves are known to significantly influence the number of bursting events (sweeps and ejections) in the wall region [12]. These sweep events are particularly important for drag reduction because they are responsible for the generation of turbulent wall shear stress [19]. Thus, drag reduction is achieved by the suppression of streamwise vortex formation [20]. Therefore, it is possible that the wave motion attenuates the formation of streaks close to the walls (bottom and/or lateral one) and in this way produces an overall reduction in skin friction. Wave-induced secondary currents can also be a way of explaining the significant enhancement of mean velocity in the bulk region when LA waves are present. Secondary currents in the liquid phase of a stratified rectangular duct flow were measured by Suzanne [13] and obtained in numerical simulations by Nordsveen [15]. In both cases, the secondary motion consisted of two big vortices in the duct cross-section area, with flow going up near the lateral walls and coming down along the duct center plane. The latter is responsible for carrying high speed fluid from the center of the duct to the wall region, possibly resulting in this way in an acceleration of the flow in the near wall region.

The described wave-induced secondary flow is evident from measurements of the mean vertical velocity, as shown in Fig. 5. For Runs 2i, 3f, and 3g, there is a mean downward flow motion, indicating the presence of wave-induced secondary motion in the middle of the duct cross-section area. The magnitude of this secondary flow is around 2–5% of the mean streamwise velocity. For Runs 2h and 3f, the flow from the interface toward the bottom of the duct is rather small as compared to that for Runs 2i and 3g. However, for these two cases, the streamwise mean velocity pro-

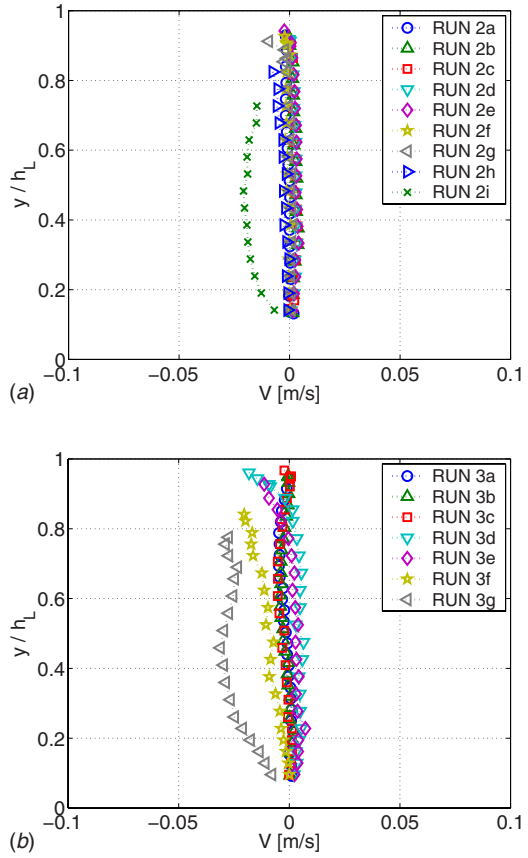

Fig. 5 Mean vertical velocity profiles for different air superficial velocities and corresponding wave patterns: (*a*) Run 2 and (*b*) Run 3. Positive mean vertical velocity implies an upward movement of the flow.

files are already significantly enhanced, as seen in Fig. 3. Therefore, some other effect rather than the secondary flow alone can be responsible for this enhancement. However, more measurements—probably with some other experimental techniques that allow for the visualization of the whole flow field in the duct cross-section area, for instance, particle image velocimetry (PIV) or simply some flow visualization technique—would be needed in order to determine the cause of this increase in bulk velocity under the presence of LA waves.

3.2 Turbulence Structure. Figures 6 and 7 show the measurements of streamwise ($u' \equiv \sqrt{\overline{u'^2}}$) and vertical ($v' \equiv \sqrt{\overline{v'^2}}$) turbulent fluctuation and Reynolds stress ($-\overline{u'v'}$) profiles for the two liquid flow rates considered.

It is seen in these figures that vertical fluctuations for the free surface flow (Runs 2a and 3a) are damped close to the wall and close to the free surface due to gravity and surface tension in the latter case. On the other hand, streamwise fluctuations peak in the near wall region, and contrary to what happens in a solid boundary, they do not vanish as the interface is approached, as expected for free-surface flows [1,3].

As the shear rate is increased, streamwise fluctuations are enhanced close to the interface (Runs 2b–2e, and 3b and 3c), while vertical fluctuations in the same region are not allowed to increase that much due to gravity and surface tension effects. Reynolds stresses for Runs 2b–2e are not affected by the applied interfacial shear or the SA waves on the interface, indicating why the mean velocity profiles for these Runs remain unaltered throughout the flow depth.

For Runs 2f and 2g, the streamwise fluctuation profiles are more similar to the unsheared interface case, with a pronounced peak as the interface is approached, giving the profile a "c" shape. The streamwise fluctuations are completely undisturbed for $y/h_L \leq 0.6$. An akin behavior is shown in the vertical intensities, where the latter are enhanced very close to the interface and remain unaltered for $y/h_L \leq 0.4$, coinciding in this region with the nonsheared case of Run 2a instead of showing a continuous deformation following Runs 2b–2e for an increasing shear rate. A sudden increase in vertical fluctuations is observed for Run 2g though, reaching a value 35% higher close to the interface than for smaller shear rates. Both streamwise and vertical fluctuations peak close to the interface just below the wave troughs. The peak magnitude increases for higher shear rates. Reynolds stresses $-\overline{u'v'}$ are decreased for both cases, with smaller values for Run 2g. For $y/h_L \leq 0.2$, turbulent intensities scale with the wall shear velocity, so that turbulence at the wall appears to be independent of what happens to the rest of the flow.

For Runs 2h and 2i, LA waves are generated by the wind shear. As a result, the bulk velocity was greatly enhanced. Streamwise turbulent intensities for these Runs peak close to the wall and just under the wave trough, apparently reducing their magnitude as the interface is approached. For higher wave amplitudes, the peak in streamwise fluctuations occurs in deeper locations and almost at the same distance down from the wave trough. Therefore, this peak is probably related to the balance between generation and dissipation of the wave-induced fluctuations as one gets away from the interface. Vertical fluctuations also peak close to the interface, decreasing their magnitude with a constant downslope until close to the wall. Here, we see how the region $y/h_L \leq 0.2$ is apparently affected by the wavy motion in both Runs. However, this is not enough reason to assume that wall turbulence and, therefore, the shear at the wall are indeed affected since measurements within the viscous sublayer would be needed to probe this assumption. Vertical fluctuations have to vanish when the wall is reached due to the physical restriction the latter imposes on the flow. The Reynolds stresses $-\overline{u'v'}$ are significantly reduced for $y/h_L \leq 0.5$ due to the LA wave motion. For Runs 2i and 3g, Reynolds stresses take a strange shape, being negative at $0.1 \leq y/h_L \leq 0.55$. In principle, the negative Reynolds stresses could be due to the fact that our experimental technique did not distinguish between wave-induced fluctuations and turbulence-induced fluctuations. The coupling between these two could be the reason for the observed negative values. At the same time, in the same depth range as the Reynolds stresses become negative, the mean velocity profile shows a negative slope, leaving the production term $-\overline{u'v'}\partial U/\partial y$ positive.

Looking at the measurements for Runs 2 and 3, the effects of applying an interfacial shear can be summarized as follows. For a free interface (open duct flow), the flow structure was similar to an open channel flow, with the mean velocity profile described by a logarithmic profile. As the interfacial shear increased, SA waves were formed on the interface. Under these conditions, the effect on the flow structure in the liquid phase was the same as that produced by an increasing shear rate on a flat interface. The wavy motion did not show any effect in the bulk flow structure, and turbulent fluctuations were enhanced continuously close to the interface as the shear increased. Mean velocity profiles were still represented by the log law of the wall. Consequently, it can be said that the interface actually acts as a flat surface with a shear imposed on it and could be treated as such in numerical simulations. These results confirm the previous suggestions by the numerical simulations of Lam and Banerjee [6], Komori et al. [4] and Lombardi et al. [21]. However, the effect of a shear imposed on the interface is restricted to the near-interface region only for low shear rates. When the shear rate was large enough to trigger a certain wave amplitude, turbulent fluctuations were suddenly enhanced close to the interface. From that moment and for increasing wave amplitudes the effect of the interface motion affected the bulk flow structure as well. Mean velocity profiles were no longer described by a logarithmic region, and turbulent fluctuations were

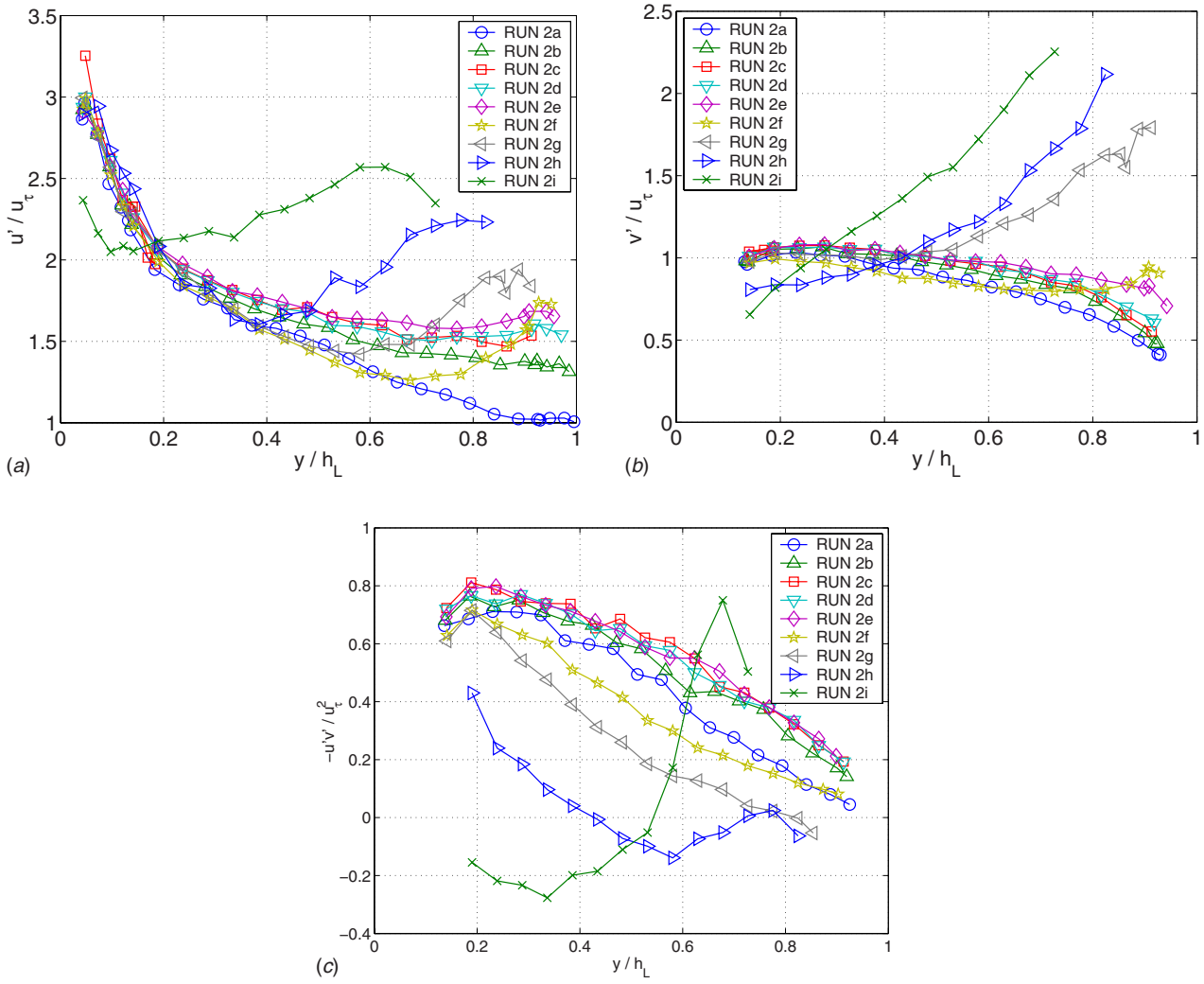

Fig. 6 Turbulent intensity profiles versus normal distance to the wall for Run 2, where $u' \equiv \sqrt{\overline{u'^2}}$ are streamwise fluctuations, $v' \equiv \sqrt{\overline{v'^2}}$ are vertical fluctuations, and $-\overline{u'v'}$ are Reynolds stresses

continuously enhanced. In both cases (for both liquid film heights considered here), the appearance of these critical waves was characterized by a wave amplitude to liquid film height ratio of approximately $h_w/h_L \geqslant 0.2$. The difference in flow structure observed before and after the appearance of these waves or of critical wave amplitudes indicates that, at some point, wave-induced fluctuations begin to be more important than turbulence-induced fluctuations. These wave-induced fluctuations could be responsible for modifying the flow structure near the bottom wall, but, again, more measurements are needed in order to try to relate the interface dynamics with the bursts and events in the wall boundary layer.

According to the previous observations, predicting the transition from a stratified smooth to a stratified wavy regime, i.e., the appearance of the first waves, is not so important as to be able to predict the emergence of the critical wave amplitudes that have a significant influence on the flow structure. The experimental technique used in this work for wave characterization [17] was not able to distinguish the appearance of this kind of waves. The technique, however, was intended to produce an objective way of characterizing the interface while velocity measurements were performed. In order to determine a more accurate technique for detecting these critical waves, more measurements of wave parameters, such as wavelength and wave amplitude, would be needed.

4 Summary and Conclusions

Streamwise mean velocity and turbulent stress profiles in the liquid phase were measured using LDV. The measurements were performed in the duct center plane, from the bottom wall to the interface. Two different liquid film heights were used, and in both cases, the effect of shear on the interface had similar results.

For a free surface (zero gas flow), the interface remained smooth, with vertical fluctuations and Reynolds stresses vanishing at the interface. The mean velocity profile was described by the log law of the wall for an open channel. SA waves resulted in an increase in the streamwise velocity close to the interface due to the higher interfacial shear rate. The latter were enhanced continuously as the gas flow rate increased, while vertical fluctuations remained close to zero in that region. This is an indication that with the presence of SA waves, the interface can still be treated as a sheared flat interface in numerical simulations. Numerical simulations found in the literature contribute to this idea by showing that treating the interface as flat with a shear imposed on it gives accurate results.

On the other hand, LA waves have a great impact on flow structure. The mean velocity showed an s-shaped profile, and the bulk velocity was increased. This apparent increase in bulk velocity was attributed either to wave-generated secondary flows or to an effect of drag reduction produced by the change in bursting

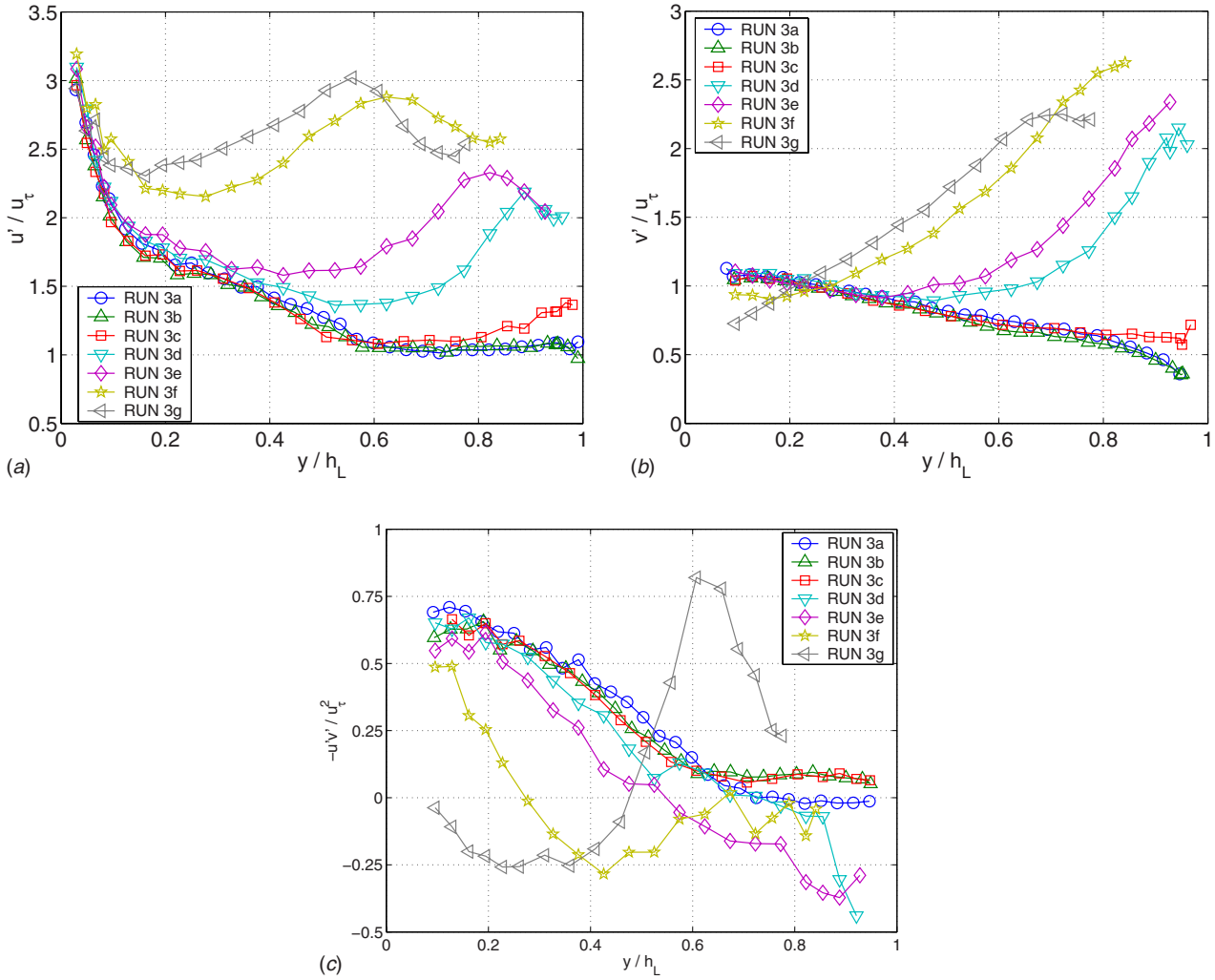

Fig. 7 Turbulent intensity profiles versus normal distance to the wall for Run 3 (wall at $y/h_L=0$, interface at $y/h_L=1$), where $u' \equiv \sqrt{\overline{u'^2}}$ are streamwise fluctuations, $v' \equiv \sqrt{\overline{v'^2}}$ are vertical fluctuations, and $-\overline{u'v'}$ are Reynolds stresses

frequency in the wall region due to the interfacial oscillations. However, this is just a hypothesis that could not be verified in the present work. More measurements, probably using another experimental technique, should be carried out in order to determine the real cause of change in the flow structure. No logarithmic region was observed in the mean velocity profile. Both streamwise and vertical fluctuations were greatly enhanced in the interface region, presenting maximum values close to the interface and close to the wall, while vertical fluctuations peaked close to the interface and decreased almost linearly to the wall. Reynolds stresses showed a completely different behavior compared to that in the SA wave regime. Their values were decreased throughout the flow depth, and some negative values were measured. Both the mean flow and turbulent stresses appeared to be modified close to the wall when LA disturbances were present. However, since the LDV measurements were performed outside the viscous sublayer, this assumption of LA waves modifying the wall turbulence could not be confirmed.

The big difference in flow structure was not observed after the appearance of the first waves but rather when a certain critical wave amplitude was triggered. Therefore, the prediction of the critical wave amplitude and wavelength, which had a significant influence on the flow and turbulence structure, seems more important than the usual determination of the transition from a smooth to a stratified wavy regime. More work should be dedicated to the characterization of this critical wave height and the prediction of its appearance.

Acknowledgment

This work was made possible, thanks to the financial support of the Norwegian Research Council through CARPET Strategic University Program.

References

[1] Nezu, I., and Rodi, W., 1986, "Open-Channel Flow Measurements With Laser Doppler Anemometer," J. Hydraul. Eng., **112**, pp. 335–355.
[2] Rashidi, M., and Banerjee, S., 1988, "Turbulence Structure in Free-Surface Channel Flows," Phys. Fluids, **31**, pp. 2491–2503.
[3] Komori, S., Ueda, H., Ogino, F., and Mizushina, T., 1982, "Turbulence Structure and Transport Mechanism at the Free Surface in an Open Channel Flow," Int. J. Heat Mass Transfer, **25**, pp. 513–521.
[4] Komori, S., Nagaosa, R., Murakami, Y., Chiba, S., Ishii, K., and Kuwahara, K., 1993, "Direct Numerical Simulation of Three-Dimensional Open-Channel Flow With Zero-Shear Gas-Liquid Interface," Phys. Fluids A, **5**, pp. 115–125.
[5] Pan, Y., and Banerjee, S., 1995, "A Numerical Study of Free-Surface Turbulence in Channel Flow," Phys. Fluids, **7**, pp. 1649–1664.
[6] Lam, K., and Banerjee, S., 1992, "On the Condition of Streak Formation in a Bounded Turbulent Flow," Phys. Fluids A, **4**, pp. 306–320.
[7] Rashidi, M., and Banerjee, S., 1990, "Streak Characteristics and Behavior Near Wall and Interface in Open Channel Flows," ASME J. Fluids Eng., **112**,

pp. 164–170.
[8] Kumar, S., Grupta, R., and Banerjee, S., 1998, "An Experimental Investigation of the Characteristics of Free-Surface Turbulence in Channel Flow," Phys. Fluids, **10**, pp. 437–456.
[9] Lorencez, C., Nasr-Esfahany, C. L. M., Kawaji, M., and Ojha, M., 1997, "Liquid Turbulence Structure at a Sheared and Wavy Gas-Liquid Interface," Int. J. Multiphase Flow, **23**, pp. 205–226.
[10] Fabre, J., Marodon, D., and Suzanne, L. M. C., 1984, *Turbulence Structure of Wavy Stratified Air-Water Flow*, Gas Transfer at Water Surfaces, W. Brutsaert and G. H. Jirka, eds., Reidel Publishing Company, Dordrecht, Holland, pp. 113–123.
[11] Kemp, P., and Simons, R., 1982, "The Interaction Between Waves and a Turbulent Current: Waves Propagating With the Current," J. Fluid Mech., **116**, pp. 227–250.
[12] Rashidi, M., Hetsroni, G., and Banerjee, S., 1992, "Wave-Turbulence Interaction in Free-Surface Channel Flows," Phys. Fluids A, **4**, pp. 2727–2737.
[13] Suzanne, C., 1985, "Structure de l'Ecoulement Stratifié de Gaz et de Liquide en Canal Rectangulaire," Ph.D. thesis, Institut National Polytechnique de Toulouse, France.
[14] Strand, O., 1993, "An Experimental Investigation of Stratified Two-Phase Flow in Horizontal Pipes," Ph.D. thesis, University of Oslo, Norway.
[15] Nordsveen, M., 1995, "Modelling of Wave and Turbulence Induced Secondary Currents in Stratified Duct Flow," Ph.D. thesis, University of Oslo, Norway.
[16] Andreussi, P., and Persen, L., 1987, "Stratified Gas-Liquid Flow in Downwardly Inclined Pipes," Int. J. Multiphase Flow, **13**, pp. 565–575.
[17] Fernandino, M., and Ytrehus, T., 2006, "Determination of Flow Sub-Regimes in Stratified Air-Water Channel Flow Using LDV Spectra," Int. J. Multiphase Flow, **32**, pp. 436–446.
[18] Fernandino, M., 2006, "Experimental and Numerical Characterization of Turbulence Structure in Stratified Horizontal Air-Water Duct Flow," Ph.D. thesis, Norwegian University of Science and Technology, Norway.
[19] Choi, K.-S., 1989, "Near-Wall Structure of Turbulent Boundary Layer With Riblets," J. Fluid Mech., **208**, pp. 417–458.
[20] Schoppa, W., and Hussain, F., 1998, "A Large-Scale Control Strategy for Drag Reduction in Turbulent Boundary Layers," Phys. Fluids, **10**, pp. 1049–1051.
[21] Lombardi, P., Angelis, V. D., and Banerjee, S., 1996, "Direct Numerical Simulation of Near-Interface Turbulence in Coupled Gas-Liquid Flow," Phys. Fluids, **8**, pp. 1643–1665.